

Combinatorial metaheuristics applied to infectious disease models

Juan José Fallas-Monge
School of Mathematics
Costa Rican Institute of Technology
Cartago, Costa Rica
Email: jfallas@itcr.ac.cr

Jeffrey Chavarría-Molina
School of Mathematics
Costa Rican Institute of Technology
Cartago, Costa Rica
Email: jchavarria@itcr.ac.cr

Geisel Alpízar-Brenes
School of Mathematics
Costa Rican Institute of Technology
Cartago, Costa Rica
Email: galpizar@itcr.ac.cr

Abstract—An experiment applying two combinatorial heuristics to three optimization problems related to infectious disease models is presented (SIR and SIS models). The study used the genetic and simulated annealing algorithms to determine the best combination for selected control measures in order to minimize the number of infected individuals and the cost of applying those measures.

Keywords: metaheuristics, simulated annealing, genetic algorithm, infectious disease, SIR model, SIS model.

I. INTRODUCTION

The study of infectious disease transmission and its control using mathematical models has become important for scientists and professionals from different areas, because of the physical and economic consequences that an infectious disease can cause in humans and animals [10]. The simulation of an infectious disease spreading in one or several populations using mathematical models allows the exploration of the results of applying control measures and this provides valuable information for decision making. Several studies have shown that mathematical models are indispensable tools for understanding the spreading dynamic of infectious diseases and the relationship between cost and efficiency when control measures are applied [9].

Two of the most popular models for studying the spread of infectious disease are SIR and SIS. In those models the size of the population is taken as a constant N , and it is divided into different groups:

- S: represents susceptibles, individuals who do not have the disease, but could be infected.
- I: Infected group, which contains people who have been infected.
- R: Recovered group, individuals who have been removed from group I. They recovered because of natural reasons or because some control mechanism, such as vaccines, was provided.

Model SIR supposes that recovered individuals have immunity against the disease (individuals from group I who have recovered are moved to group R). This model could be appropriate for infectious diseases caused by viruses such as measles, mumps and smallpox [10]. On the other hand, the SIS model moves recovered people from I to S. This means people could

be infected again because of lacking immunity. The SIS model could be used to simulate diseases caused by bacteria, such as meningitis and sexually transmitted diseases.

The SIR model discrete equations are shown in (1), where $\gamma > 0$ is a recovery rate, that is, the probability that an infected individual is moved from group I to group R, in a time interval Δt . Furthermore, $\alpha > 0$ is a contact rate (related to the number of contacts sufficient to transmit the disease). Then $\frac{\alpha \Delta t S_n}{N}$ represents the average of contacts that one infected person has had with individuals from group S during that period of time. Finally, $\frac{\alpha \Delta t S_n}{N} I_n$ is the number of individuals who change from group S to I at time n .

$$\begin{aligned} S_{n+1} &= S_n - \frac{\alpha \Delta t S_n}{N} I_n \\ I_{n+1} &= I_n - \gamma \Delta t I_n + \frac{\alpha \Delta t S_n}{N} I_n \\ R_{n+1} &= R_n + \gamma \Delta t I_n, \end{aligned} \quad (1)$$

with $S_0 > 0$, $I_0 > 0$, $R_0 \geq 0$, and such that $S_0 + I_0 + R_0 = N$. Also, equations (2) show how the numbers of susceptible and infected individuals are updated in the SIS model at time n . In this case, $S_0 > 0$, $I_0 > 0$ and $S_0 + I_0 = N$.

$$\begin{aligned} S_{n+1} &= S_n - \frac{\alpha \Delta t S_n}{N} I_n + \gamma \Delta t I_n \\ I_{n+1} &= I_n - \gamma \Delta t I_n + \frac{\alpha \Delta t S_n}{N} I_n \end{aligned} \quad (2)$$

Both models determined by equations (1) and (2) simulate the infectious disease spreading without any control measure. Section I-A explains how the SIR and SIS models can be modified and used to simulate the spreading, considering selected controls against the disease.

A. SIR and SIS discrete models with control measures

Based on [5], the equations in (3) show how the SIR model could be written, considering a treatment. In this case, u is the proportion of individuals treated at time k , β is the transmission rate, and d_2 is the death rate.

$$\begin{aligned} S_{k+1} &= S_k(1 - u) - \beta(S_k(1 - u))I_k \\ I_{k+1} &= I_k + \beta S_k(1 - u)I_k - d_2 I_k \\ R_{k+1} &= R_k + u S_k \end{aligned} \quad (3)$$

On the other hand, based on [4] an SIS model with one treatment measure can be proposed. Equations (4) show how to update the numbers of susceptible and infected individuals in this model.

$$\begin{aligned} S_{k+1} &= \gamma G_k S_k + \gamma(1 - \sigma\tau)I_k \\ I_{k+1} &= \gamma(1 - G_k)S_k + \gamma\sigma\tau I_k, \end{aligned} \quad (4)$$

where $G_k = \exp\left(\frac{-\alpha I_k}{N_k}\right)$ is the probability of remaining susceptible from time k to $k+1$, α is a weighting constant to control the prevalence of $\frac{I_k}{N_k}$ (infected proportion at time k), and $N_k = S_k + I_k$. Furthermore, if γ is a survival probability, then $\gamma G_k S_k$ is the number of individuals that remain susceptible at time $k+1$, and $\gamma(1 - G_k)S_k$ is the number of individuals that change from group S to group I . Finally, $(1 - \sigma)$ is a recovery rate (without treatment) and $(1 - \tau)$ is a recovery rate because of treatment.

These models describe the spreading dynamic of an infectious disease in one population. Based on equations (3) and (4) other SIR and SIS models can be considered if the spreading occurs between two or more interconnected populations.

B. Population models

Population models allow the understanding of how migration affects the spreading of an infectious disease. They consider migration, without forgetting the residence patch, as well as the patch in which one person is located in a given time [3]. In this research two interconnected populations, denoted x and y , are considered, in which individuals are homogeneously distributed. Equations (5) represent the SIR discrete model, based on [8], for two patches x and y (in fact, the model includes eight equations, in this case equations for patch x are shown, the remaining equations could be written changing x to y).

$$\begin{aligned} S_{k+1}^{xx} &= (1 - \rho_S^{xy})(S_k^{xx} - \beta S_k^{xx}(I_k^{xx} + I_k^{yx})) + \\ &\quad \tau_S^{yx}(S_k^{xy} - \beta S_k^{xy}(I_k^{xy} + I_k^{yy})) \\ S_{k+1}^{xy} &= (1 - \tau_S^{xy})(S_k^{xy} - \beta S_k^{xy}(I_k^{xy} + I_k^{yy})) + \\ &\quad \rho_S^{xy}(S_k^{xx} - \beta S_k^{xx}(I_k^{xx} + I_k^{yx})) \\ I_{k+1}^{xx} &= (1 - \rho_I^{xy})(I_k^{xx} + \beta S_k^{xx}(I_k^{xx} + I_k^{yx}) - dI_k^{xx}) + \\ &\quad \tau_I^{yx}(I_k^{xy} + \beta S_k^{xy}(I_k^{xy} + I_k^{yy}) - dI_k^{xy}) \\ I_{k+1}^{xy} &= (1 - \tau_I^{xy})(I_k^{xy} + \beta S_k^{xy}(I_k^{xy} + I_k^{yy}) - dI_k^{xy}) + \\ &\quad \rho_I^{xy}(I_k^{xx} + \beta S_k^{xx}(I_k^{xx} + I_k^{yx}) - dI_k^{xx}) \end{aligned} \quad (5)$$

In this model, for $A \in \{S, I\}$, A_k^{xy} indicates how many individual from group A and patch x are located in y , at time k . Furthermore, ρ_A^{xy} is the emigration rate from x to y , and τ_A^{xy} is the immigration rate from y to x . A similar interpretation can be made for A_k^{yx} and τ_A^{yx} . Also, β is the transmission rate and d is an attrition rate. Finally, fluctuations for β are not considered, because migration number is considered small compared to the population size.

If a population with two patches is considered, with the local dynamic in each patch modeled by the equations (4), then the SIS model could be adapted to simulate how an infectious disease evolves in both patches, taking into account the migration. Let S_k^x and I_k^x , respectively, be the groups of susceptible and infected individuals at time k in patch x . In patch x people survive with probability γ^x , meanwhile the infected individuals recovered for natural reasons with probability $(1 - \sigma^x)$. Furthermore, the susceptible get infected according to the rate $(1 - G_k^x)$. Finally, a fraction $(1 - \tau^x)$ from the infected group is removed and returned to the group S_k^x because they were treated. Thus, the local dynamic in each patch can be modeled by equations (6).

$$\begin{aligned} \tilde{S}_k^x &= \gamma^x G_k^x S_k^x + \gamma^x(1 - \sigma^x \tau^x)I_k^x \\ \tilde{I}_k^x &= \gamma^x(1 - G_k^x)S_k^x + \gamma^x \sigma^x \tau^x I_k^x, \end{aligned} \quad (6)$$

If the migration between x and y is considered, then D_S^z and D_I^z , with $z \in \{x, y\}$, are the fractions of susceptible and infected individuals moving at each period of time. Therefore, the SIS model for one population with two patches is defined by equations (7).

$$\begin{aligned} S_{k+1}^x &= (1 - D_S^x)\tilde{S}_k^x + D_S^y\tilde{S}_k^y \\ I_{k+1}^x &= (1 - D_I^x)\tilde{I}_k^x + D_I^y\tilde{I}_k^y, \\ S_{k+1}^y &= D_S^x\tilde{S}_k^x + (1 - D_S^y)\tilde{S}_k^y, \\ I_{k+1}^y &= D_I^x\tilde{I}_k^x + (1 - D_I^y)\tilde{I}_k^y, \end{aligned} \quad (7)$$

II. THE OPTIMIZATION PROBLEMS

The optimization problems studied in this research will be presented. The SIR model was adapted to study the spreading of an infectious disease when control measures were applied. First, the SIR model was used to simulate the spreading in one population (SIR1P), and then in two interconnected populations (SIR2P). Also, a third problem was explored using the SIS model in two populations with selected control measures (SIS2P).

In the case of SIR1P, the optimization problem was based on the functional (8) presented in [5], which was considered together with the equations (3), changing u to u_k , that is the proportion of people that will be treated at the time k .

$$\sum_{k=1}^{T-1} (I_k + Bu_k^2 + B_1 u_k) + I_T, \quad (8)$$

where T is number of time periods that will be modeled. Furthermore, $k \in \{0, 1, \dots, T-1\}$ and the restrictions $0 \leq u_k \leq 1 - d$ and $0 \leq d \leq 1$ are considered. Additionally, B and B_1 are coefficients that represent the cost of applying the control measure u_k .

On the other hand, the optimization problem for SIR2P is formulated using the emigration and immigration rates of infected individuals as the control measures. The vectors

$$\rho_I^{xy} = (\rho_{I_0}^{xy}, \rho_{I_1}^{xy}, \dots, \rho_{I_{T-1}}^{xy}) \quad \text{and} \quad \tau_I^{xy} = (\tau_{I_0}^{xy}, \tau_{I_1}^{xy}, \dots, \tau_{I_{T-1}}^{xy})$$

are used to track at time k the movement of infected individuals between the patches, with $k \in \{0, 1, \dots, T-1\}$. In this case the functional (9) is used together with the equations (5), but changing τ_I^{yx} to $\tau_{I_k}^{yx}$, and ρ_I^{yx} to $\rho_{I_k}^{yx}$. The idea is to take control of the number of infected people that are moving from one patch to another. Also, τ_S^{yx} and ρ_S^{yx} are constant rates, and the restrictions $0 \leq \tau_I^{yx} \leq \tau_S^{yx}$ and $0 \leq \rho_I^{yx} \leq \rho_S^{yx}$ are used.

$$\sum_{x,y} \left[\sum_{k=1}^{T-1} \left(B_1 \left(\hat{I}_k^x \right)^2 + B_2 \left(\tau_{I_k}^{yx} - \tau_S^{yx} \right)^2 + B_3 \left(\rho_{I_k}^{yx} - \rho_S^{yx} \right)^2 \right) + \left(\hat{I}_T^x \right)^2 \right], \quad (9)$$

where $\hat{I}_k^x = \frac{I_k^{xx} + I_k^{yx}}{N_k^x}$, which represents the prevalence of infected individuals in group x at time k , with N_k^x the population size of patch x at that time. Also, B_i , for $i = 1, 2, 3$, are relative costs, such that if $B_1 = 1$, then B_2 is the cost of applying restrictions to the infected individuals that are returning to x , and B_3 is the cost of applying restrictions to the infected individuals that are leaving x .

In the third case, for model SIS2P, the functional (10) is used together with the equations (6) and (7).

$$\sum_{x,y} \left[\sum_{k=1}^{T-1} \left(B_1 \left(\hat{I}_k^x \right)^2 + B_2 \left(f_k^x \right)^2 + B_3 \left(1 - \tau_k^x \right)^2 + B_4 \left(D_{I_k}^x - D_S^x \right)^2 \right) + \left(\hat{I}_T^x \right)^2 \right] \quad (10)$$

such that at (6) the parameter G_k^x is defined by $G_k^x = \exp \left(\frac{-\alpha(1-f_k^x)I_k}{N_k} \right)$. In this model the control was applied at time k to:

- the rates $D_{I_k}^x$ and $D_{I_k}^y$, that represent the proportion of infected individuals that will be allowed to move from x to y , and reciprocally.
- the variable τ_k^x , where $1 - \tau_k^x$ is the proportion of people which will be treated in patch x .
- the parameter f_k^x , which is related to the social distance, that is the percentage of infected individuals that will be separated from susceptible individuals.

In all three models, the main goal is to minimize the cost functional according to the equations of each model. This process minimizes at the same time the number of infected individuals and the cost of applying the control measures.

III. THE HEURISTICS

For the genetic algorithm (GA) (see Algorithm [A]) a population of $M = 15$ instances is used, and the stationary state model mentioned in [2] was used, that is in the selection step some instances from the current population can be part of the next. The initial population was built randomly and the population size increases during the crossover and decreases to $M = 15$ with the selection. Furthermore, the selection step is based on the *stochastic universal sampling* strategy presented in [12].

The model SIR1P uses for each instance only one control vector U , whereas that SIR2P uses for each instance four vectors: $\rho_I^{xy}, \rho_I^{yx}, \tau_I^{xy}$, and τ_I^{yx} . Finally, the model SIS2P uses six vectors: $D_I^x, D_I^y, \tau^x, \tau^y, f^x$ and f^y . All the control vectors are of size T . Depending on the number of vectors in each model, the crossover process with probability p_c was made with one or two cut points. The model SIR1P uses two cut points (see Figure 1) and both models SIR2P and SIS2P use only one cut point.

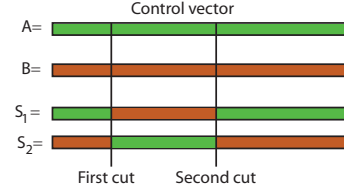


Fig. 1. Two cut points strategy for the crossover process.

For each instance the mutation occurs with probability p_m . When an instance is selected to mutate, for each control vector of that instance one position is chosen randomly. That entry is modified by adding the number $0.001 \cdot n$, where $n \in \mathbb{N}, n \leq 10$, chosen randomly. The step size 0.001 was selected due to the numerical calculations, designed using three significant digits. In this study the probabilities of crossover and mutation are estimated via experimentation (see Section IV). Also, more than *maxiter* iterations are not made if in those iterations there is no change in the best solution registered in memory. For SIR1P *maxiter* = 30, for SIR2P *maxiter* = 150, and for SIS2P *maxiter* = 300. These values were selected depending on the complexity of each model (for instance, the model SIR1P uses the functional (8) and equations (3), which required fewer iterations compared to the model SIR2P which uses the functional (9) and the equations (5)). Each value represents the minimum number of iterations that should be executed to guarantee a good performance in the respective algorithm.

[A] Algorithm GA

- 1) Initial population is built with 15 instances. The fitness is calculated according to the model (using the respective functional).
- 2) Let $\Psi(t) := \{P^1, \dots, P^{15}\}$.
- 3) Initialize t and *auxiter* at 0.
- 4) $BestFitness := +\infty$.
- 5) Repeat while *auxiter* \leq *maxiter*
 - a) Increment t and *auxiter*.
 - b) Apply crossover operator with probability p_c .
 - c) Apply mutation operator with probability p_m .
 - d) Select $\Psi(t+1)$ from $\Psi(t)$ by a random roulette process (SUS).
 - e) If one instance P^n from $\Psi(t)$ improves the best fitness in memory, then
 - i) Let $BestFitness := P^n.fitness$
 - ii) Reset *auxiter* to 0.
- 6) Return the best instance in memory.

On the other hand, the simulated annealing algorithm (SA) (see algorithm [B]) is based on the Metropolis' rule in order to decide whether a new feasible solution (a neighbor for the current solution) is accepted or not. The initial temperature T^* was calculated using an acceptance rate χ_0 (see [1]) and the final temperature (T_f) was fixed at 0.00001.

[B] Algorithm SA

- 1) $s :=$ initial random solution.
- 2) $T^* :=$ initial temperature calculated with $\chi_0 = 0.96$.
- 3) Initialize k at 0.
- 4) Repeat while $T_k > T_f$
 - a) Increment k .
 - b) Do L_T times
 - i) $s' :=$ Build a neighbor for s .
 - ii) Let $\Delta E := s.\text{fitness} - s'.\text{fitness}$
 - iii) If $\Delta W < 0$ do $s := s'$, otherwise do $s := s'$ with probability $\exp(-\Delta W/T^*)$.
 - c) Let $T_{k+1} := \alpha \cdot T_k$.
- 5) Return s .

The solutions in simulated annealing were represented by vectors of size T , as in the genetic algorithm the instances were encoded (one vector for SIR1P, four vectors in SIR2P, and six vectors for SIS2P). Finally, the process to build a neighbor (see step (4i) in algorithm [B]) was inspired by the mutation process previously described for the GA algorithm.

IV. INITIAL CONDITIONS AND PARAMETERS FITTING

In GA the parameters p_c and p_m were analyzed. Both parameters were studied from 0 to 1, using a step of 0.05. For each combination of p_c and p_m , 500 multistart runs were made and a performance percentage was calculated. With those percentages, and for each model, a contour map was built in order to visualize the behavior of the genetic algorithm. The fitness values were calculated using the functions (8), (9) or (10), depending on the model.

First, based on [5] the following initial conditions were used for the SIR1P model: $N = 105$, $I(0) = 5$, $R(0) = 0$, $T = 10$, $B = 20$, $B_1 = 1$, $\beta = 0.02$, $d_2 = 0.01$, and $d = 0.2$. Under these conditions, the reference value for the fitness was 144.660452399522 (required to calculate the performance percentage). Figure 2 shows the performance of the genetic algorithm in the SIR1P. Based on these results both probabilities were fixed for this model at 0.95.

Second, for SIR2P the following initial conditions were used: $S^{xx} = 1500$, $S^{yy} = 1000$, $I^{xx} = 1$, $S^{xy} = S^{yx} = I^{yy} = I^{xy} = I^{yx} = 0$, $B_1 = 1$, $B_2 = 0.2$, $B_3 = 0.2$, $\tau_S^{xy} = \rho_S^{xy} = 0.03$, $\tau_S^{yx} = \rho_S^{yx} = 0.02$, $\beta = 0.001$, $d = 0.44$, and $T = 15$ ([5], [6], [7],[11]). The reference value for the fitness in this experiment was 4.52338522907883. Figure 3 shows the performance of the genetic algorithm in the SIR2P model. In this case, the range of possibilities for both parameters is larger. Several combinations can be chosen, in particular the pair (p_c, p_m) can be taken such that $(p_c, p_m) \in [0.85, 1] \times [0.4, 0.85]$. Therefore, in this study

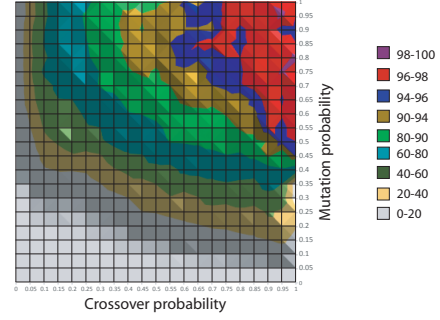


Fig. 2. Contour map for SIR1P in GA.

and for the SIR2P model the combination $p_c = 0.95$ and $p_m = 0.55$ was selected.

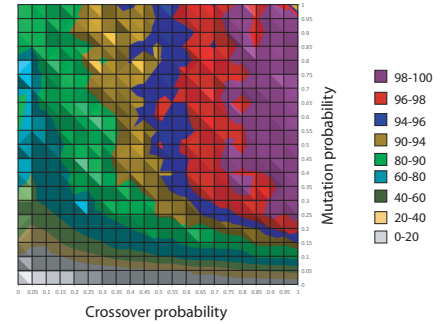


Fig. 3. Contour map for SIR2P in GA.

Then, for the model SIS2P: $S^x = S^y = 1500$, $\gamma^x = \gamma^y = 1$, $\sigma^x = \sigma^y = 6/7$, $D_S^x = D_S^y = 0.03$, $B_1 = 1$, $B_2 = 0.04$, $B_3 = 0.004$, $B_4 = 0.0004$, $f^x \in [0, 0.2]$, $f^y \in [0, 0.2]$, $D_I^x \in [0.001, D_S^x]$, $D_I^y \in [0.001, D_S^y]$, $1 - \tau^x \in [0, 0.05]$, and $1 - \tau^y \in [0, 0.05]$. The reference value for the fitness was 50.2170566977095. Figure 4 shows the results and justifies the combination $p_c = 0.95$ and $p_m = 0.35$ as the selected values in this model. Table I summarizes the crossover and mutation probabilities selected depending on the model.

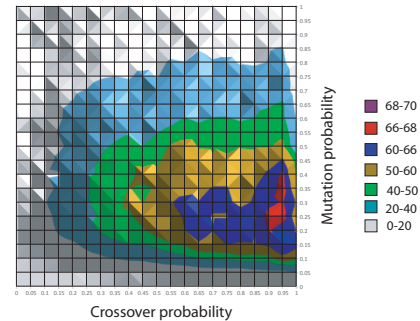


Fig. 4. Contour map for SIS2P in GA.

A similar experiment was developed for the simulated annealing algorithm, using the same initial conditions previously described for each model in the GA algorithm. The initial temperature T^* was calculated using $\chi_0 = 0.96$ (acceptance

TABLE I
CROSSOVER AND MUTATION PROBABILITIES SELECTED DEPENDING ON
THE MODEL.

	SIR1P	SIR2P	SIS2P
p_c	0.95	0.95	0.95
p_m	0.95	0.55	0.35

rate) and $T_f = 0.00001$ (the final temperature). For each combination of α values (this parameter was analyzed for $\alpha \geq 0.95$) and for each model, 500 multistart runs were executed and the performance percentage was calculated. For instance, Figure 5 shows how the performance percentage increases, in the SIR2P model, according to α values closer to one. In this model, a 100% performance was achieved for $\alpha \geq 0.9935$. Because α represents the cooling rate in SA, and the execution time increases for larger values of α , then for the SIR2P model this parameter was fixed at $\alpha = 0.9935$ (the minimum value required to achieve the 100% performance).

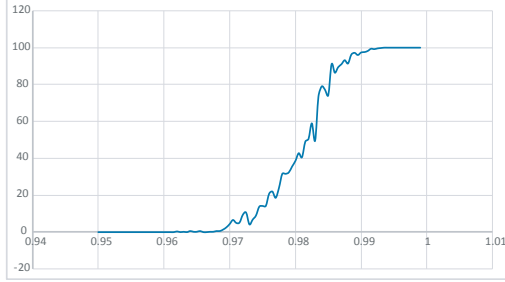


Fig. 5. Performance percentage versus α values in SA.

The parameter L_T is the length of the Markov chain and it was selected depending on the complexity of the model. Table II summarizes the selected values for L_T and it shows for each model the minimum value for α (the cooling rate in SA) required to achieve a 100% performance with the SA algorithm.

TABLE II
LENGTH OF THE MARKOV CHAIN AND RANGES FOR α .

	SIR1P	SIR2P	SIS2P
L_T	30	100	300
$\alpha \geq$	0.985	0.9935	0.999

Finally, Table III shows the mean and the standard deviation of the total number of fitness evaluations for each algorithm (in 1000 multistart runs). The simulated annealing algorithm always uses the same number of evaluations because all the executions use the same initial temperature and a fixed final temperature to stop the algorithm. On the other hand, the genetic algorithm stops if there is no change in the best solution registered in memory after *maxiter* iterations are made. Due to this stop criterion, the total number of fitness evaluations is not constant for the genetic algorithm.

TABLE III
MEAN AND STANDARD DEVIATION OF THE NUMBER OF FITNESS
EVALUATIONS FOR EACH MODEL.

	Meanx	Standard deviation
GA-SIR1P	138005	29900
GA-SIR2P	131275	20106
GA-SIS2P	874533	60320
SA-SIR1P	105801	0
SA-SIR2P	108299	0
SA-SIS2P	3653724	0

V. NUMERICAL RESULTS

Table IV shows the average times calculated for the heuristics in each model. Also the standard deviation and the performance are included. The results for SIR1P and SIR2P show that the average time for SA is less compared to the average time for the GA algorithm. Also, in both cases the SA algorithm had better performance. On the third case, GA has less average time, but its performance was almost duplicated for SA.

Summarizing, the experiment showed that SA has better qualities than GA to study the optimization problems formulated in this paper. The SA algorithm was shown to be faster and excellent performance percentages were obtained.

TABLE IV
TIME AND PERFORMANCE OF GA AND SA ALGORITHMS ON THE MODELS.

SIR1P		
	GA	SA
Time		
Avg (s)	0.522797	0.319579
SD	0.089870	0.009224
Performance	99.9%	100%
SIR2P		
	GA	SA
Time		
Avg (s)	1.255823	0.950631
SD	0.199491	0.011273
Performance	78.1%	99.9%
SIS2P		
	GA	SA
Time		
Avg (s)	17.294875	23.168199
SD	1.237952	0.268691
Performance	49.4%	99.8%

On the other hand, Figures 6, 7 and 8 show how the number of the infected individuals changes in each model according to the best solution and the worse combination for the control measures. Furthermore, the cost for both combinations is indicated. The worse case occurs when in all periods of time:

- the proportion of treated people in model SIR1P is taken equal to zero.

- the migration rates for the infected individuals in model SIR2P are taking constant and equal to the rates for susceptible individuals.
- the dispersion rates (D_I^x and D_I^y) in the SIS2P model are constant and take the maximum value, equal to the rates for susceptible individuals. Furthermore, no individuals are treated and the infected individuals are not separated from the susceptible individuals.

The results showed how the optimization process found the best combination for the control measures, and the experiment achieved to minimize the number of infected individuals, together with the minimization of the cost of applying the measures.

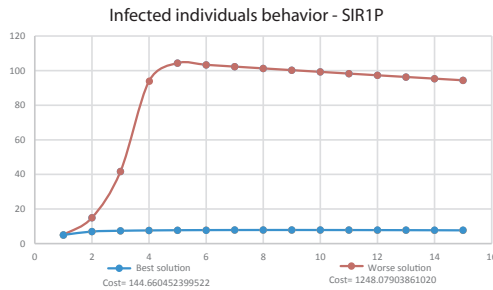


Fig. 6. Change of the number of infected individuals for the best solution and the worse case for the model SIR1P.

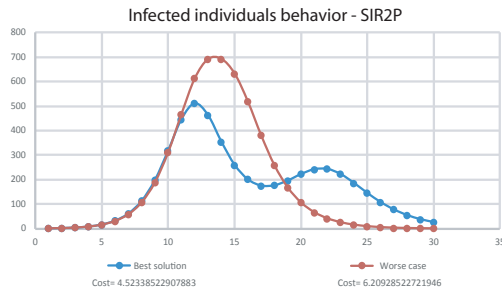


Fig. 7. Change of the number of infected individuals for the best solution and the worse case for the model SIR2P.

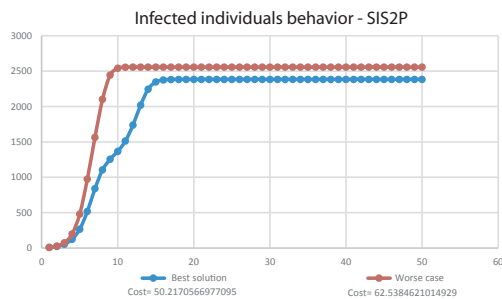


Fig. 8. Change of the number of infected individuals for the best solution and the worse case for the model SIS2P.

VI. CONCLUDING REMARKS

The experiment showed how the simulated annealing algorithm presented better characteristics to study the optimization

problems formulated in order to minimize the number of infected individuals and the cost of applying control measures, when the spreading of an infectious disease is modeled with the SIR and SIS models, and according to the cost functional presented in each case.

Furthermore, the study showed how the control measures are necessary to regulate the spreading of the disease and to take control over the cost. If control measures are not applied the number of infected individuals increases and the cost of taking care of them is higher, compared with any other scenario.

On the other hand, the parameter fitting made with both heuristics strengthened the hypothesis concerning how the performance of a heuristic algorithm depends strongly on the values assigned to its parameters. In particular, the fitting process showed that the mutation probability in GA is not generalizable to all spreading disease models. It was necessary to use a high value for the SIR1P model, but smaller values were used for SIR2P and SIS2P models. Finally, it was clear in the fitting process that values close to 1.0 are required for the cooling rate (α) to have good results in the simulated annealing algorithm.

Acknowledgments: The authors were supported with project 5401-1440-4201 of the Research Vice Rectory, Costa Rica Institute of Technology.

REFERENCES

- [1] Aarts, E. & Korst, J. (1990). Simulated annealing and boltzmann machines: A stochastic approach to combinatorial optimization and neural computing. John Wiley & Sons, Chichester.
- [2] Abbass, H.; Sarker, R. & Newton, C. (2002). Data mining: A heuristic approach. Idea Group Publishing, Hershey.
- [3] Arino, J. & Driessche, P. (2006). "Disease spread in metapopulations", Fields Institute Communications 48(1): 1-13.
- [4] Castillo-Chavez, C. & Yakubu, A. (2002). "Intraspecific competition, dispersal and disease dynamics in discrete-time patchy environments", Mathematical Approaches for Emerging and Reemerging Infectious Diseases: An Introduction to Models, Methods and Theory 125(1): 165-181.
- [5] Ding, W. & Lenhart, S. (2010). "Introduction to optimal control for discrete time models with an application to disease modeling", DIMACS Series in Discrete Mathematics and Theoretical Computer Science 75: 109-119.
- [6] González, P.; Lee, S.; Velázquez, L. & Castillo-Chavez, C. (2011). "A note on the use of optimal control on a discrete time model of in uenza dynamics", Mathematical Biosciences and engineering 8: 183-197.
- [7] Herrera-Valdez, M.; Cruz-Aponte, M. & Castillo-Chavez, C. (2011). "Multiple outbreaks for the same pandemic: local transportation and social distancing explain the diferent waves of ah1n1pdm cases observed in mexico during 2009", Mathematical Biosciences and engineering 8: 21-48.
- [8] Keeling, M. & Rohani, P. (2002). "Estimating spatial coupling in epidemiological systems: a mechanistic approach", Ecology Letters 5: 20-29.
- [9] Kretzschmar, M. & Kretzschmar, J. (2010). Mathematical models in infectious disease epidemiology", in: A. Kramer; M. Kretzschmar & K. Krickeberg (Eds.), Modern Infectious Disease Epidemiology, Springer, Berlin: 214-226.
- [10] Ma, S. & Xia, Y. (2009). Mathematical understanding of infectious disease dynamics. World Scientific, Singapore.
- [11] Murray, J. (2001). Mathematical biology. Springer, 3 edition.
- [12] Talbi, E. (2009). Metaheuristics: From design to implementation. John Wiley & Sons, New Jersey.